Peer-reviewed version available at *Appl. Sci.* **2020**, *10*, 4777; doi:10.3390/app10144777

Article

Underwater Optical Path Loss after Passage of Tropical Storm

Peter C. Chu *, and Chenwu Fan

Naval Ocean Analysis and Prediction Laboratory, Department of Oceanography, Naval Postgraduate School; pcchu@nps.edu

* Correspondence: pcchu@nps.edu; Tel.: (1-831-656-3688)

Abstract: Underwater wireless optical communications (UWOC) have attracted considerable attention in recent years as an alternative means for acoustic communication. However, optical path loss of light propagation from attenuation is large due to absorption and scattering in various water conditions. Identification of environmental effects especially tropical storms on underwater optical path loss is the key to the success of using optics for UWOC. Underwater inherent optical properties (IOPs) such as the beam attenuation coefficient for 470 nm light in the western North Pacific Ocean were measured from the U.S. Naval Oceanographic Office sea gliders with being deployed after Super Typhoon Guchol (7-20 June 2012)'s passage during 25-30 June 2012 and no any typhoon passage during 9 January – 28 February 2014. The observed two sets (with and without super typhoon) of IOPs are taken as input into a recently developed Radiative Transfer Equation solver. The simulated normalized received powers for the two durations show large impact of typhoon passage on UWOC.

Keywords: underwater wireless optical communication (UWOC); radiative transfer equation solver; optical path loss; tropical cyclone.

1. Introduction

Optical beam propagation is a challenge in underwater wireless optical communication (UWOC) due to scattering and absorption in complicated water bodies varying from deep oceans to shallow water with limiting the propagation of the optical beam [1]. For example, dissolved mineral components, colored organic matter, and salts are found in clear ocean water. High concentration of suspended particles and dissolved minerals are found in turbid harbors. Underwater turbulence is another challenge. The fluctuations in the temperature, salinity, and density caused by the atmospheric forcing lead to huge fluctuations in the intensity of the signal at the receiver. Besides, interference and dispersion must also be taken into account for UWOC problems. The underwater channel is much more complex in comparison to free space optics. The pure water has 1000 times the attenuation of clear air and turbid water has more than 100 times the attenuation of the densest fog. Therefore, one of the main challenges in UWOC channel modeling is to evaluate the overall underwater optical path loss under severe weather conditions.

Three types of communication links are available: line of sight, modulating retro reflector, and reflective. The line of sight link is the straight and unobstructed path of communication between transmitter and receiver. The modulating retro reflector link has optical communication and other functions such as programmable signage using an optical retro reflector and an optical modulator. The reflective communication link has transmitter to emit light upward towards the air-ocean interface with an inclination angle greater than the critical angle to ensure total internal reflection.

The optical path loss from the transmitter to receiver directly determines the quality of the line of sight link.

Tropical storms especially typhoons/hurricanes generate strong surface wind stress that enhances the currents, waves, and turbulences, and in turn changes the absorption and scattering of the water and constituents within, such as particles of various origins, including algal cells, detritus, sediments, plankton, and even bubbles near the surface, cause the significant optical path loss. Particle scattering, path radiance, and turbulence affected by the atmosphere are dominant factors in power reduction in UWOC [3]. Little attention has been paid to the effects of typhoon/hurricane 's passage on optical path loss, despite evidence suggesting that the strong winds significantly affect underwater inherent optical parameters (IOPs) such as beam attenuation coefficient [3], and in turn the quality of UWOC [4]. This may be caused that the tropical storm is not a typical phenomenon in the area where UWOC links are used. However, study on the path loss after the typhoon passage is useful for UWOC since we may want to know how many days do we need to wait to use UWOC again. Investigation of optical path loss (directly affecting the line of sight link) after typhoon passage in comparison to that without typhoon passage shows the typhoon effect.

Recently, a direct radiative transfer equation (RTE) solver was developed on the base of the Gauss-Seidel iterative method [5] to compute the received power of UWOC systems. Unlike uniform discretization of the angular space as in [6], an optimal non-uniform angular discretization scheme is used to consider the strong forward scattering characteristics of ocean waters. After angular discretization, an upwind type finite-difference method is applied to discrete space, and the Gauss-Seidel iterative method is used to solve the fully discretized large system of linear algebraic equations. We used this RTE solver to obtain the path loss for the two sets of IOPs with and without typhoon passage. Since the optical path-loss from transmitter to receiver directly affects the line of sight link, we calculate the optical path-loss with and without typhoon passage using the RTE solver to identify typhoon effect on the UWOC line of sight link.

The rest of the paper is outlined as follows. Section 2 describes the selection of typhoon influence area. Section 3 describes IOPs in the western Pacific Ocean observed by the Naval Oceanographic Office (NAVOCEANO) Seagliders with and without typhoon passage. Section 4 depicts a two-dimensional RTE. Section 5 shows the impact of typhoon's passage on the optical path loss. Section 6 presents the conclusions.

2. Selection of Typhoon Influenced Area

Typhoons hit the western North Pacific Ocean from early June to early December in 2012 and early March to early December in 2014 [7]. To study the typhoon's effect on UWOC, ideally the IOP data should be collected from measurements that are taken at the same geographic location directly before and after a storm event since the influence of hydrography, land, and seasonal variability cannot be ignored. However, such practice is difficult due to the basic features of tropical storm and the difficulty in IOP observation. Tropical storms typically form over large bodies of relatively warm water and span a large range of sizes, from 100 to 2,000 kilometers as measured by the radius of vanishing wind [7]. Average life of a hurricane, determined by time and place of origin and rate of forward movement, is 9 days. The longest life cycle of a hurricane ever recorded was Tropical Cyclone Ginger, which lasted 31 days (September 5 to October 5, 1971) [8].

To overcome such a difficulty, we choose a typhoon influenced area with high ocean transparency with low seasonal variability. The Secchi Disk depth (SDD) is a key index of water transparency. The satellite observations by the Sea-Viewing Wide Field-of –View Sensor (SeaWiFS) show the global climatological annual

mean and absolute seasonal amplitude (maximum minus minimum) of SDD [9]. The area [124°E-134°E, 15°N-27°N] is characterized as high transparency with low seasonal variability from Fig. 3 and Fig. 4 of [9].

In 2012, a tropical disturbance formed south-southeast of Pohnpei on June 7, and was upgraded to a tropical depression on June 10 in the area [124°E-134°E, 15°N-27°N]. The system later intensified in favorable conditions, and reached typhoon intensity (i.e., Typhoon Guchol) on June 15. It reached super typhoon status on June 16-17, before making landfall over Japan as a typhoon on June 19 (Fig. 1). Guchol brought heavy rain and strong winds in the Western Pacific Ocean near Japan on June 19 and 20. On the contrary, there was no typhoon activity in the Western Pacific Ocean during 6 January – 28 February 2014 [7]. The IOPs were measured from Seagliders of the Naval Oceanographic Office (NAVOCEANO) during two different periods: (a) 25-30 June 2012, which is 7 days after super Typhoon Guchol 's passage, and (b) 9 January – 28 February 2014 with no typhoon activities.

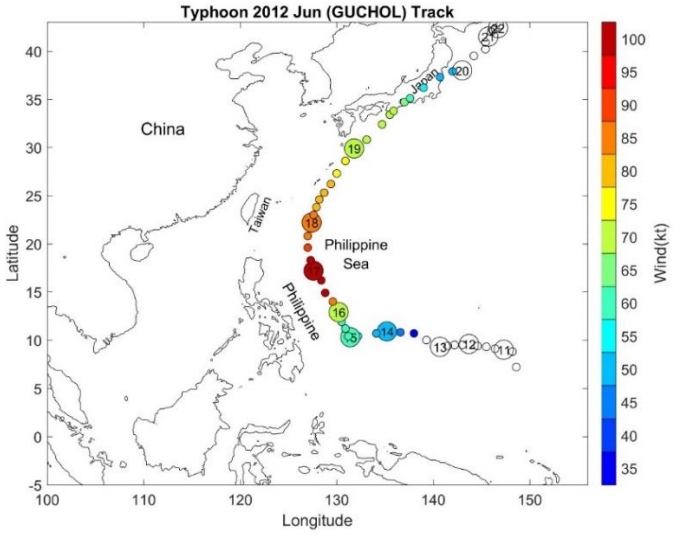

Figure 1. Geography of the Western Pacific Ocean and track of super typhoon Guchul-2012 with strength.

3. IOPs with and without Typhoon Passage

The glider is a remote operator programmed to perform a series of downward and upward tracks while collecting various oceanographic parameter data using various installed sensor packages. It can position itself at the ocean surface with a 45° downward angle to present the antenna array skyward to facilitate two-way satellite communications. The NAVOCEANO Seaglider has the Seabird Electronics SBE 41 CP CTD sensor (hydrographic measurement) and WET Lab s' Beam Attenuation Meter (BAM) (optical measurement) [10]. The technical details about the BAM can be found in [11]. The Seaglider measures temperature, salinity, and beam attenuation coefficient (c) down to 100 m depth. NAVOCEANO has routine quality control procedures on the all raw observational data. Bad profiles were removed due to obviously erroneous location, large spikes, and mismatch of characteristics with the surrounding profiles.

NAVOCEANO provided the profile data of three Seagliders inside the area [124°E-134°E, 15°N-27°N] after quality control with high transparency and low seasonal variability. Among them two Seagliders (NG226, NG232) were in the area where super Typhoon Guchol was passing by 7 days ago. The two Seagliders were deployed from a survey ship 15 minutes and 223 m apart: UTC 03:19, 25 June 2012 at (25°30'20"N, 131°59'51"E) for NG226 (blue trajectory in Figs. 2a, b), and UTC 03:34, 25 June 2012 at (25°30'27"N, 131°59'55"E) for NG232 (red trajectory in Figs. 2a, b). The two Seagliders took very different trajectories despite

they were very close (only 223 m apart) initially with NG226 drifting southwestward and then southward and NG232 drifting southeastward and then northeastward. On 30 June 2012, NG226 was located at (24°59'27"N, 131°59'26"E) on UTC 17:24; however, NG232 was located at located at (25°34'50"N, 132°10'20"E) on UTC 17:51. Such strong bifurcation of ocean currents was generated at the wake of super Typhoon Guchul. The third Seaglider (NG270) was underwater during 6 January – 28 February 2014 without any typhoon activities (magenta trajectory in Fig. 2a). We use IPO data from the two Seagliders or comparison: NG226 with typhoon and NG270 without typhoon.

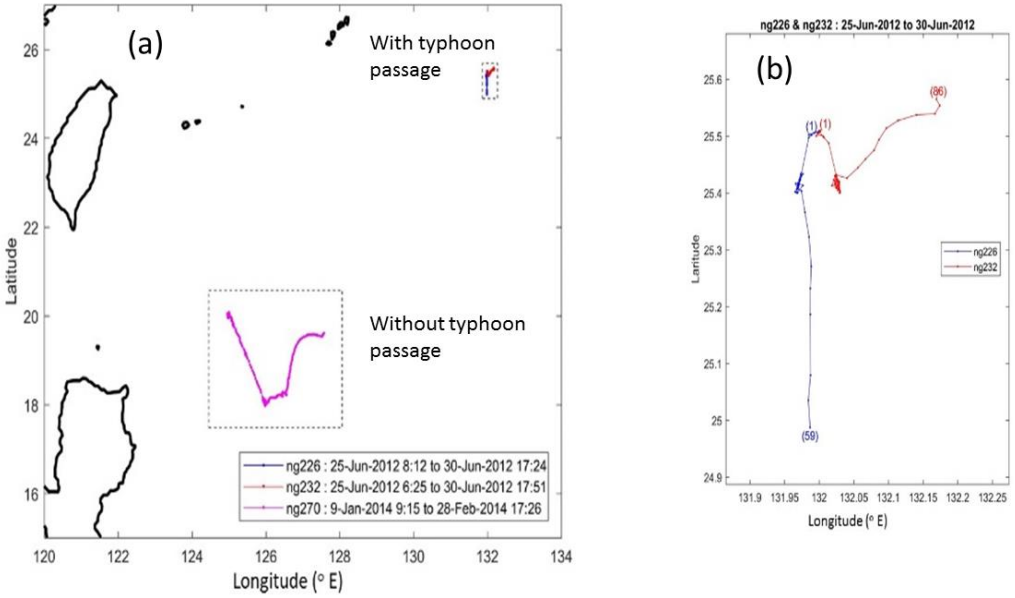

Figure 2. Tracks of (a) NAVOCEANO Seagliders NG270 during 9 Jan – 28 Feb 2014 (red) without typhoon activity, as well as zoomed-in view of tracks of Seagliders (NG226, NG232) during 25-30 Jan 2012 (blue) after super typhoon Guchol 's passage, and (b) zoomed-in view of (NG226, NG232).

The beam attenuation coefficient c (470 nm) measured by NG 226 (59 profiles) during June 25-30, 2012 after super Typhoon Guchol passage (Fig. 3) are large with horizontally averaged values (red solid profiles) generally greater than 0.8 m^{-1}. The beam attenuation coefficient c (470 nm) measured by NG 270 (825 profiles) during 6 January – 28 February 2014 with no typhoon activity (Fig. 4) is much smaller with horizontally averaged values less than 0.05 m^{-1}.

Preprints (www.preprints.org) | NOT PEER-REVIEWED | Posted: 7 June 2020 doi:10.20944/preprints202006.0077.v1

Peer-reviewed version available at Appl. Sci. 2020, 10, 4777; doi:10.3390/app10144777

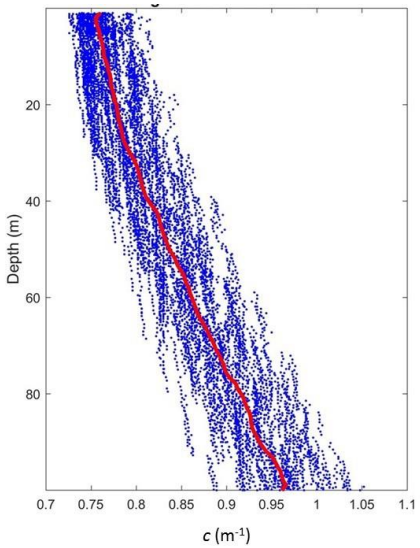

Figure 3. Beam attenuation coefficient c (470 nm) profiles collected from glider NG 226 (59 profiles) June 25-30, 2012 (after super Typhoon Guchol passage). The red solid profiles are horizontally averaged values generally larger than 0.8 /m[1].

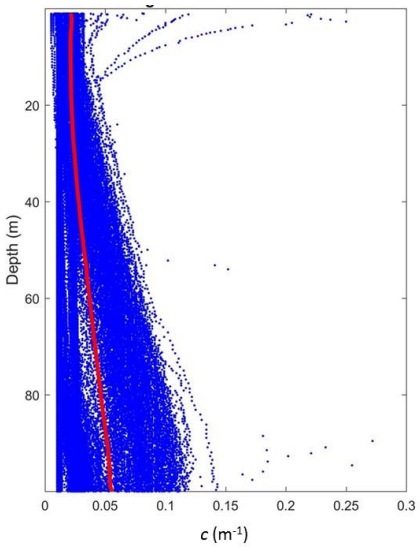

Figure 4. Beam attenuation coefficient c (470 nm) profiles collected from glider NG 270 (825 profiles) 6 January – 28 February 2014 with no typhoon activity. The red solid profiles are horizontally averaged values generally smaller than 0.05/m.

Difference of $c(z)$ between Figure 3 and Figure 4 is huge. During super Typhoon Guchol passage, high winds generated strong upwelling in the upper ocean and pumped rich nutrients upward from the subsurface layer to the euphotic layer. This would induce the phytoplankton chlorophyll-*a* (Chl-*a*) to breed and grow rapidly. The Chl-*a* concentration (C) is directly related to the beam attenuation coefficient by a classical least-square fitted formula for the wavelength of 490 nm [12],

$$c(z) = c_w(z) + 0.39\left[C(z)\right]^{0.57} \quad (1)$$

where $c_w(z)$ is the beam attenuation coefficient for the pure water. If we assume that Eq (1) is also valid for the wavelength of 470 nm, the IOP measurements (Figures 3 and 4) show the abundance of Chl-*a* after typhoon passage.

4. Two-dimensional RTE

Let the optical beam axis point in the *z*-direction (i.e., light propagation direction) with ρ the radial coordinate, **n** the unit vector representing the projection of direction of light vector onto the transverse plane, **n'** the corresponding scattered direction. Let θ be the scattering angle between **n** and **n'**, i. e., $\mathbf{n} \bullet \mathbf{n}' = \cos\theta$. Here, θ is the scattering angle. An asymmetry parameter g (ranging from 0 to 1) describes scattering types with $g = 0$ for dominating isotropic scattering and g near 1 for peaked scattering. The value of g is near 0.924 for the sea water [13], which indicates the feasibility for underwater optical communication. Scattering and absorption are azimuthally symmetric when they are independent on the azimuthal angle. The phase function is [14]

$$\beta(\mathbf{n}, \mathbf{n}') = \frac{1-g^2}{2\pi(1+g^2-2g\cos\theta)} \tag{2}$$

for the azimuthally symmetric scattering. For the azimuthally symmetric scattering and absorption, the radiance, $L(\mathbf{r}, \mathbf{n})$ [Watts/(m^{2}sr)], is independent on the azimuthal angle. Under the small-angle approximation and negligible temporal dispersion, the RTE is a differential-integral equation with the position vector $\mathbf{r} = (\rho, z)$, and the direction vector **n** are two-dimensional [5]

$$\mathbf{n} \bullet \nabla L(\rho, z, \mathbf{n}) = -cL(\rho, z, \mathbf{n}) + b\int_{2\pi} \beta(\mathbf{n}, \mathbf{n}')L(\rho, z, \mathbf{n}')d\mathbf{n}' + S(\rho, z, \mathbf{n}) \tag{3}$$

which has three independent variables, ρ, z, and θ. Since the observational beam attenuation coefficient is in vertical (z) with resolution of approximately 1 m, the position coordinates (ρ, z) are discretized into (1 m × 1 m) grids,

$$\rho_i = i\Delta\rho, \quad z_j = j\Delta z, \quad \Delta\rho = \Delta z = 1 \text{ m}. \tag{4}$$

The angular variable θ is discretized into K (=72) directions with equal angle interval (5°),

$$\theta_k = k\Delta\theta, \quad \Delta\theta = 5^o. \tag{5}$$

The differential-integral equation (3) is discretized into a set of algebraic equations,

$$\sin\theta_k \frac{L_{i,j,k} - L_{i-1,j,k}}{\Delta\rho} + \cos\theta_k \frac{L_{i,j,k} - L_{i,j-1,k}}{\Delta z} + c_j L_{i,j,k} = b_j \sum_{k'=1}^{K} w_{k,k'} L_{i,j,k'} + S_{i,j,k}, \quad b_j = \omega c_j \tag{6}$$

where $w_{k,k'}$ is the discretized phase function (2); and c_j is the observed beam attenuation coefficient. Following [5] with the same discrete phase function $w_{k,k}$, the Gauss-Seidel iteration is used to solve the discrete 2D RTE (6),

$$L_{i,j,k}^{l+1} = \frac{\frac{\sin\theta_k}{\Delta\rho} L_{i-1,j,k}^{l+1} + \frac{\cos\theta_k}{\Delta z} L_{i,j-1,k}^{l+1} + b_j \sum_{k'=1}^{K} w_{k,k'} L_{i,j,k'}^{l} + S_{i.j.k}}{\sin\theta_k / \Delta\rho + \cos\theta_k / \Delta z + c_j} \tag{7}$$

where I is the iterative step. The iteration is repeated until the relative error norm is smaller than a predetermined termination value (10^{-4}) [5],

$$\frac{\sum_i \sum_j \sum_k \left[L_{i,j,k}^{l+1} - L_{i,j,k}^{l} \right]^2}{\sum_i \sum_j \sum_k \left[L_{i,j,k}^{l} \right]^2} < 10^{-4} \quad (8)$$

Let R be the radius of the receiver aperture. The scattering is assumed symmetric in the azimuthal direction, which means that the radiance for any azimuthal angle on the same circle is the same. Therefore, the received power can be defined as lateral integration of the radiance at z [5]

$$P(z) = \int_{2\pi} \int_0^R L(z, \rho, \theta) \rho d\theta d\rho = \sum_{m=1}^{M} A_m \left[\sum_{k=1}^{K} L_{m+(I-1)/2, J, k} \Delta\theta_k \right] \quad (9)$$

where $A_1, A_2, \ldots, A_M$ are the areas of the circular regions with θ from 0 to 2π, and ρ from 0 to Δρ/2 (A_1), from Δρ/2 to 3Δρ/2 (A_2), …, from Δρ/2+(m-2)Δρ to Δρ/2+(m-1)Δρ (A_m), until m = M=R/Δρ, i.e.,

$$A_1 = \pi \left(\frac{\Delta\rho}{2} \right)^2, \quad A_m = \pi \left[\frac{\Delta\rho}{2} + (m-1)\Delta\rho \right]^2 - \pi \left[\frac{\Delta\rho}{2} + (m-2)\Delta\rho \right]^2, m = 2, 3, ..., M \quad (10)$$

The normalized received power

$$P_n(z_j) = P(z_j) / P(z_0) \quad (11)$$

is used to represent the optical power loss. Here, z_0 is the source depth. Since we only have beam attenuation coefficient data, it is hard to conduct link budget and system analysis for optical communication. As a first step, we calculate the optical power loss using the RTE solver to identify indirectly the performance of the optical communication (line of sight) link.

5. Effect of Super Typhoon Guchul's Passage

With the beam attenuation coefficient $c(z)$ collected from three NAVOCEANO 's Seagliders depicted in Section 3, the volume back scattering coefficient $b(z)$ is calculated with a single scattering albedo, $\omega = b/c$. The light albedo (ω) for light with wavelength of 514 nm is 0.241 for the clear ocean, 0.551 for the coastal ocean, and 0.833 for a turbid harbor. At 470 nm, ω would be higher and less variable because lower absorption than at 514 nm [15]. Thus, the value of ω is selected as 0.75, an average between 0.60 (>0.551) and 0.90 (>0.833) for our study area (western North Pacific). Between the two Seagliders, NG226 was under super Typhoon Guchul 's influence (see Fig. 2b and Fig. 3) and NG270 was not (see Fig. 2a, and Fig. 4). We assume that there no natural optical source, i.e., $S = 0$. It is noted that the same albedo is used for all cases. It seems likely that a storm event will change the composition of the scattering and absorbing water constituents and hence the albedo. We will study this issue in near future.

In the simulation, the light propagation direction (z) is assumed vertically downward since the IOP data in vertical. The model parameters are taken as: z_j the same as the observational depth of the individual Seaglider 's profile with Δz nearly 1 m and the source depth at the first observational point; the lateral step size Δρ = 0.01 m; the receiver aperture = 0.1 m; and $K = 32$. The Gauss-Seidel iteration (4) is used to solve the 2D RTE (3) with observed beam attenuation coefficient $c(z_j)$ and calculated volume back scattering coefficient $b(z_j)$

Preprints (www.preprints.org) | NOT PEER-REVIEWED | Posted: 7 June 2020 doi:10.20944/preprints202006.0077.v1

Peer-reviewed version available at Appl. Sci. 2020, 10, 4777; doi:10.3390/app10144777

with a single albedo ω=0.75 to obtain the radiance $L_{I,j,k}$ and in turn to calculate the normalized received power $P_n(z)$.

The cross sections of the beam attenuation coefficient $c(z)$ during 6 Jan – 28 Feb 2014 without typhoon activity along the track of the NAVOCEANO Seaglider NG270 (Fig. 5a) show small values c < 0.05 m^{-1}. The corresponding normalized received power $P_n(z)$ reduces slowly from 1 at the surface to 0.1-1 at 40 m (Fig. 5b), which indicates the feasibility of using UWOC without strong events like typhoon. Usually, an UWOC link can be as long as 20 m. The minimum received optical power of -19 dBm is required to achieve a bit-error rate (BER) of 1.0 $\times 10^{-3}$ to establish a 9-m underwater optical channel at 1 Gbps.

On the other hand, the cross section of the beam attenuation coefficient c(z) during 25-30 Jan 2012 after super typhoon Guchol 's passage along the tracks of the NAVOCEANO Seaglider NG226 (Fig. 6a) shows large values $c > 0.75$ m^{-1}. The corresponding normalized received power $P_n(z)$ reduces rapidly from 1 at the surface to 10^{-10} at z = 40 m along NG226 (Fig. 6b). This indicates that super typhoon Guchol l destroyed the UWOC even after 7 to 13 days passage.

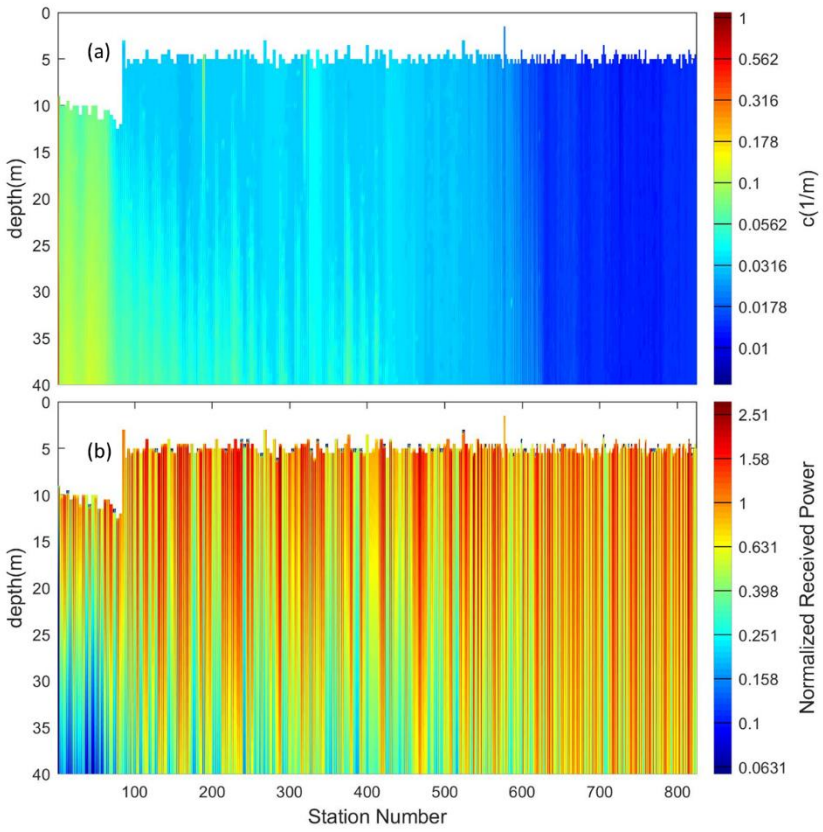

Figure 5. (a) Cross-section of observed volume attenuation coefficient $c(z)$ along the tracks of NAVOCEANO Seaglider NG270 during 6 Jan – 28 Feb 2014 (red) without typhoon activity, and (b) calculated normalized received power $P_n(z)$. The horizontal axis shows the glider's location along the magenta-colored track in Fig. 4a with Station-1 located at (19°36'32"N, 124°58'56"E) on 05:01 UTC, 09 January 2014 and Station-825 (19°59'27"N, 127°34'05"E) at 17:26 UTC, 28 February 2014. Note that there was no typhoon passing by during that period.

Preprints (www.preprints.org) | NOT PEER-REVIEWED | Posted: 7 June 2020 doi:10.20944/preprints202006.0077.v1

Peer-reviewed version available at Appl. Sci. 2020, 10, 4777; doi:10.3390/app10144777

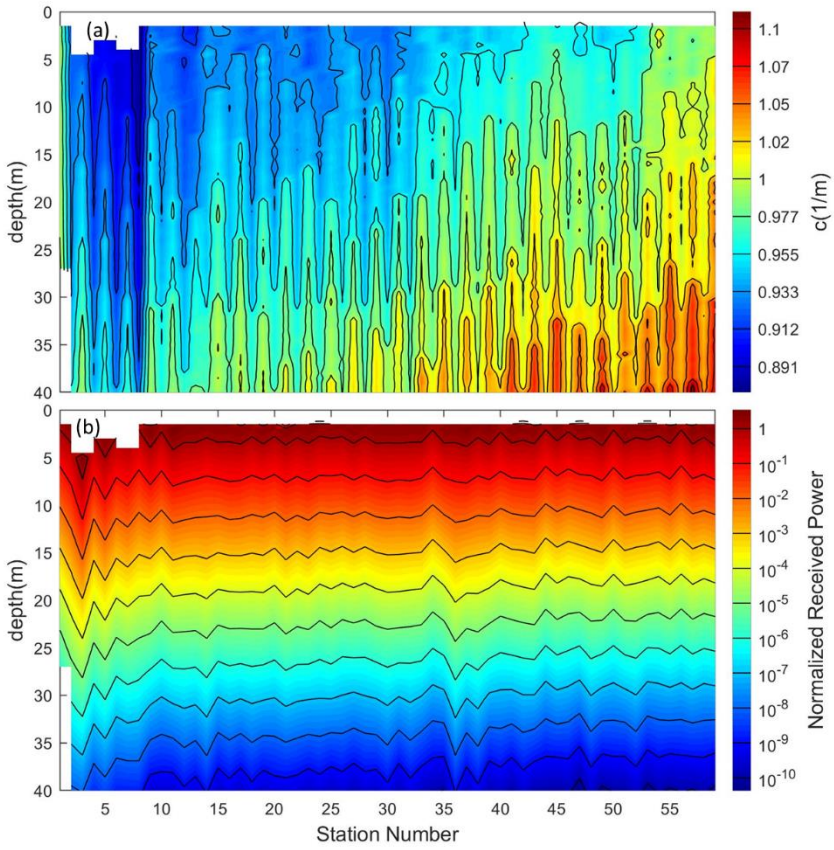

Figure 6. (a) Cross-section of observed volume attenuation coefficient c(z) along the tracks of NAVOCEANO Seaglider NG226 during 25-30 Jan 2012 after super typhoon Guchol 's passage, and (b) calculated normalized received power $P_n(z)$. The horizontal axis shows the glider's location along the blue-colored track in Fig. 4b with Station-1 located at (25°30'20"N, 131°59'51"E) on UTC 03:19, 25 June 2012 and Station-59 (24°59'27"N, 131°59'26"E) at UTC 17:24, 30 June 2012. It is noted that the super Typhoon Guchol moved out the area on 18 June 2012.

6. Conclusions

This study identifies the typhoon effects on UWOC in the western North Pacific Ocean solving a 2D RTE numerically with the data collected by three NAVOCEANO Seagliders. The beam attenuation coefficient c (470 nm) were measured during June 25-30, 2012 after super Typhoon Guchol passage and during 6 January – 28 February 2014 with no typhoon activity. Huge difference was found in the horizontally averaged c with greater than 0.8 m^{-1} during Typhoon Guchol 's passage and with much smaller values less than 0.05 m^{-1} without typhoon activity. The volume back scattering coefficient $b(z)$ is calculated from the observed beam attenuation coefficient $c(z)$ with a single scattering albedo ω=0.75. The 2D H-G phase function is used for the azimuthally symmetric and strong forward scattering with g = 0.924. After discretization in position and direction, the 2D RTE becomes a set of algebraic equations. The Gauss-Seidel iteration is used to solve the 2D RTE and in turn to calculate the normalized received power using observed IOPs from the NAVOCANO Seagliders with and without the influence of typhoon. The simulated results show that the super typhoon Gochul destroyed the UWOC due to the rapid reduction of the normalized power from 1 at the surface to 10^{-10} at z = 40 m, in comparison to 1.0 to 0.1 at z = 40 m without typhoon passage.

The results only show the strong typhoon effect through comparison between NG226 and NG270 during the two periods: June 25-30, 2012 and 6 January – 28 February 2014. These two short durations

are not enough to conclude and affirm the feasibility of using UWOC in Western North Pacific Ocean without typhoon passage because it is well known that the IOPs of the underwater channel can be easily affected by phenomena such as wind, surface waves, optical turbulences, water currents, etc. Furthermore, the actual UWOC analysis is thin here since developing a full communication system model is beyond the scope of the current effort. The communication link performance has not been evaluated due to limited data available. It will be investigated in future studies using more complete dataset and UWOC link models.

Author Contributions: conceptualization, P.C.; methodology, P.C.; software, C.F.; validation, C.F.; formal analysis, P.C.; investigation, C.F.; resources, P.C.; data curation, C.F.; writing—original draft preparation, P.C.; writing—review and editing, P.C.; visualization, C.F.; supervision, P.C.; project administration, P.C.; funding acquisition, P.C.

Funding: This research was funded by the Office of Naval Research.

Acknowledgments: We thank the Naval Oceanographic Office for the use of optical data from three Seagliders.

Conflicts of Interest: The authors declare no conflict of interest.

References

1. R. C. Smith, and K. S. Baker, ``Optical properties of the clearest natural waters (200800 nm)," Appl. Opt., **1981**, 20 (2), 177-184.
2. W. Hou, E. Jarosz, S. Woods, W. Goode, and A. Weidemann, ``Impacts of underwater turbulence on acoustical and optical signals and their linkage," Opt. Exp., **2013**, 21 (4), 4367-4375.
3. P. C. Chu, and C.W. Fan, "Underwater optical detection after passage of tropical storm," J. Appl. Remote Sens. 13(4), 047502 (2019), doi: 10.1117/1.JRS.13.047502.
4. P.C. Chu, B. F. Breshears, A. J. Cullen, R. F. Hammerer, R. P. Martinez, T. Q. Phung, T. Margolina, and C.W. Fan, "Environmental effects on underwater optical transmission," Ocean Sensing and Monitoring IX, edited by Weilin (Will) Hou, Robert A. Arnone, Proc. of SPIE Defense and Security, Anaheim, California, USA, 8-13 April **2017**, Vol. 10186, doi: 10.1117/12.2256466.
5. C. Li, and K.-H. Park, "On the use of a direct radiative transfer equation solver for path loss calculation in underwater optical wireless channels," IEEE Wireless Commun. Lett., **2015**, 4 (5), 561-564.
6. H. Gao and H. Zhao, "A fast-forward solver of radiative transfer equation," Transp. Theory Statist. Phys., **2009**, 38 (3), 149–192.
7. Wikipedia, "Tropical cyclone," https://en.wikipedia.org/wiki/Tropical_cyclone **2019**.
8. University of Rhode Island, "Hurricanes, science and society," http://hurricanescience.org/science/science/hurricanelifecycle/ **2019**.
9. X. He, D. Pan, Y. Bai, T. Wang, C. A. Chen, Q.. Zhu, Z. Hao, and F. Gong, "Recent changes of global ocean transparency observed by SeaWiFS," Cont. Shelf Res., **2017**, 143, 159-166.
10. K. L Mahoney., K. Grembowicz, B. Bricker, S. Crossland, D. Bryant, and M. Torres, "RIMPAC 08: Naval Oceanographic Office glider operations," Proc SPIE Defense and Security, Orlando, Florida, USA, 29 April **2009**, 7317:731706. doi: 10.1117/12.820492.
11. S. Garaba, I. Joshi, and Zaneveld, R., "Technical report on Wetlabs AC-S absorption and beam attenuation meter," Maine Insitu Sound and Color Lab, the University of Maine, Technical Report, 1-14, ftp://misclab.umeoce.maine.edu/users/optics/classFTP2013/Final_Projects/GroupSIA/Dummies_Intro_ACS_SG.pdf **2013**.
12. K.J. Voss, "A spectral model of the beam attenuation coefficient in the ocean and coastal waters," Limnol. Oceangr., **1992**, 37 (3), 501-509.

13. M. Gabriel, A. Khalighi, S. Bourennane, P. Léon, and V. Rigaud, "Monte-Carlo-based channel characterization for underwater optical communication systems," J. Opt. Commun. Netw., **2013**, 5 (1), 1–12.

14. L. G. Henyey, and J. L. Greenstein, "Diffuse radiation in the galaxy," Astrophys. J., **1941**, 93, 70-83.

15. C. Mobley, "Ocean Optics Web Book," **2016**, http://www.oceanopticsbook.info/